Molecular profiles of the mouse postnatal development of the esophageal epithelium showing delayed growth start

HIROYUKI DAIKO[1,2], NORIYUKI ISOHATA[1,3], MASAYUKI SANO[1], KAZUHIKO AOYAGI[1], KENJI OGAWA[3], SHINGO KAMEOKA[2], TERUHIKO YOSHIDA[1] and HIROKI SASAKI[1]

[1]Genetics Division, National Cancer Center Research Institute, Tsukiji 5-1-1, Chuo-ku, Tokyo 104-0045; [2]Department of Surgery II, School of Medicine, Tokyo Women's Medical University, 8-1, Kawadacho, Shinjuku-ku, Tokyo 162-8666; and [3]Medical Center East, School of Medicine, Tokyo Women's Medical University, 1-10, Nishiogu 2-chome, Arakawa-ku, Tokyo 116-8567, Japan

Received July 24, 2006; Accepted September 18, 2006

Abstract. Studies on molecular mechanisms of self-renewal in normal stem cells are required for understanding the cancer stem cell. Self-renewal in many kinds of normal stem cells might be accelerated in the growth of a young organism and in the repair of damaged tissue. This study examined whether the esophagus in growing neonates provides an experimental system for studies on epithelial stem cell renewal. The esophageal epithelium consists of 3 layers, from the luminal side to the bottom: the differentiated, epibasal and basal cell layers. The basal cell layer is known to contain the stem cells for the esophageal epithelium. This basic architecture is observed both in mice and humans. We investigated the basal cells in the mouse neonate by immunostaining with a basal cell marker, nerve growth factor receptor (Ngfr), and compared the basal cell content in the esophageal epithelium between mice and humans. A mouse esophageal epithelial cell primary culture system was developed for studies on the basal cell growth and keratinocyte differentiation, and microarray analysis was conducted for obtaining expression profiles of the basal cells. It was revealed that the growth of the esophageal epithelium begins from postnatal day 3, and that the timing is consistent with membrane localization of Ngfr in the basal cell. An increase in the basal cell number by Ngf treatment is observed in *in vitro* mouse esophageal epithelium cultures. Furthermore, mRNA overexpression of *Pdgfrb* encoding platelet derived growth factor receptor ß and *Egfr* encoding epidermal growth factor receptor is associated with the timing of the growth of the esophageal epithelium in the neonatal mice. This study provides a new experimental model for studies on the growth of the basal cells, which are considered to include the stem cells, and on the enlargement of the body size in young organisms.

Correspondence to: Dr Hiroki Sasaki, Genetics Division, National Cancer Center Research Institute, 1-1, Tsukiji 5-chome, Chuo-ku, Tokyo 104-0045, Japan
E-mail: hksasaki@gan2.res.ncc.go.jp

Key words: esophagus, epithelium, nerve growth factor, microdissection, microarray

Introduction

There is increasing evidence supporting the cancer stem cell hypothesis (1-5). Normal stem cells in the adult organism are for tissue renewal, are immortal, and rather resistant to drugs. They are able to differentiate and form specific types of tissue by asymmetrically producing two daughter cells; a new stem cell, and a progenitor cell, which has differentiation and proliferation ability, but no capability for self-renewal. Cancer stem cells might be derived from self-renewing normal stem cells due to altered proliferative pathways or from progenitor cells that have acquired the ability of self-renewal. In both cases, dysregulation of stem cell self-renewal is a key event in tumorigenesis. Therefore, studies on the molecular mechanisms of self-renewal in normal stem cells are required for cancer stem cell research. Self-renewal in many kinds of normal stem cells might be accelerated in the growth of a young organism and in the repair of damaged tissue. But much remains to be learned on stem cell renewal in growing neonates. Furthermore, molecular biological study on the enlargement of the body size in young organisms has rarely been found.

The esophagus may be one of the most simple organs. The luminal surface of the human esophagus is linked by a non-keratinizing, stratified squamous epithelium. Histologically, the esophageal epithelium can be divided into three layers: a single basal cell layer that adheres to the basement membrane (the basal cell layer), a variable number of small basophilic cell layers above this (the epibasal cell layers), and multiple layers of progressively flattened, differentiated squamous cells (the differentiated cell layers) (6,7). Cell proliferation is limited to the basal layer and the epibasal layers, from which cells are thought to migrate towards the lumen side. In general, stem cells are thought to be not only self-renewing but also slowly or rarely cycling. However, most of the basal cells actively proliferate and are thus considered to be transit amplifying cells, and only a limited number of the basal cells

Table I. PCR primer sequences.

Gene	Forward primers	Reverse primers
Krt14	5'-CCAATTCTCCTCATCCTCT-3'	5'-TCTTCCAGCAGTATCTGCGT-3'
Krt15	5'-TGAGTTGCAGTCTCAGCTCA-3'	5'-CCAATACCAGCCATCTTAGC-3'
Itga1	5'-AAGCAGACCTGCTGTTCATC-3'	5'-CCATCTCTCCATGGATAGAC-3'
Itgb1	5'-TCGTGCATGTTGTGGAGACT-3'	5'-GAGCTTGATTCCAATGGTCC-3'
Itgb4	5'-AGGGTATCATCACCATCGAG-3	5'-TTATGGTTCCTGGACAGCAC-3'
Ngfr	5'-ATTGCTCCATCTTGGCTGCT-3'	5'-ATTGAGCAGCTTCTCGACCT-3'
Pdgfrb	5'-ATGAGAGGAAGATGCTGACG-3'	5'-GTAGGACTCGAGATAACCCA-3'
Egfr	5'-GAACATCACCTGTACAGGCA-3'	5'-TCTGGGTACGTTCAATGGCA-3'
Robo1	5'-GCTCTGTGACTGTAGGTTTC-3'	5'-GCTAATTTGAAGAAGCCCCA-3'
Actin	5'-CTACAAATGTGGCTGAGGAC-3	5'-CACAGAAGCAATGCTGTCAC-3'

are stem cells. Thus, esophageal epithelial cell differentiation follows a unidirectional linear pathway from the stem cells to the transient amplifying cells in the basal cell layer, and thence to the epibasal cells, and finally to the differentiated cell.

During the process of establishing a mouse esophageal epithelial cell culture system, we discovered that esophageal epithelium growth begins from postnatal day 3, and that the timing is consistent with membrane localization of nerve growth factor receptor Ngfr and mRNA overexpression of *Pdgfrb* (platelet derived growth factor receptor ß) and *Egfr* (epidermal growth factor receptor) in the basal cells. The basal cell number was increased by Ngf treatment in *in vitro* mouse epithelium cultures. This study provides a new experimental model for studies on the growth of the basal cells, which include esophageal epithelial stem cells and on the enlargement of the body size in young organisms.

Materials and methods

Immunohistochemistry. For immunohistochemical staining of frozen sections of murine esophagus, specimens that were embedded in a TissueTek OCT medium (VWR Scientific, Torrance, CA) and stocked at -80˚C until use were cut into 5-μm sections, which were then immediately fixed in 100% ethanol for 2 min. Blocking was carried out with the Vector M.O.M. kit (for antibody made in mouse, BMK-2202; Vector Laboratories, Burlingame, CA), and the Dako protein block (for others, X0909; Dako, Carpinteria, CA) for 30 min at room temperature. Sections were incubated overnight at 4˚C with diluted rabbit polyclonal antibody directed against mouse Ngfr (ab8875, 1:50; Abcam, Cambridge, MA), and rat monoclonal antibody directed against Integrin b1 (Itgb1) (558741, 1:50; BD Biosciences, San Jose, CA). On the following day, after washing sections with PBS containing 0.1% Tween-20, endogenous peroxidase activity was blocked with 3% H_2O_2 in methanol for 30 min. Biotinylated secondary antibodies were applied for 30 min at room temperature. Detection was carried out with the Vectastain ABC Elite kit (PK-6100; Vector Laboratories). After extensive rinsing and incubation with an avidin-biotin immunoperoxidase complex, staining was visualized with the DAB system (Nichirei, Tokyo, Japan), and the sections were counter-stained with Mayer's hematoxylin.

The primary culture of mouse esophageal epithelial cells. On early postnatal days 1-7, the esophagi of the 57BL/6J mice were minced, then suspended and sterilized with 10% antibiotic-antimycotic (Invitrogen, Carlsbad, CA), and digested by incubation for 12 min at 37˚C in 0.05% collagenase1 (Nitta Gelatine, Osaka, Japan), and then manually dissociated with scissors, and incubated for 5 min at 37˚C with a 1:1 ratio of 0.5% Trypsin-EDTA (Invitrogen) and Dispase 10000PU (Godo Shusei, Tokyo, Japan) in PBS (-). Following filtration with a 100-μm cell strainer (Falcon, Franklin Lakes, NJ), the digested tissue fragments were centrifuged for 5 min at 1,200 rpm, resuspended in Defined Keratinocyte-SFM (Invitrogen) with 1 ml of supplement and antibiotic-antimycotic, plated in type 1 collagen-coated 35-mm culture dishes (Iwaki, Tokyo, Japan) and incubated at 37˚C in a humidified atmosphere flushed with 5% CO_2 in the air. Twenty-four hours after plating, non-adhesive cells were discarded. The culture medium was changed every other day. For Ngf treatment, 2 μg/ml of recombinant mouse Ngf (13257-019; Invitrogen) was added.

Immunostaining of mouse primary cultured cells. Cultured cells were fixed in 4% paraformaldehyde for 20 min and permeabilized in 0.3% TritonX-100 for 10 min at room temperature. Blocking was carried out with the Vector M.O.M. kit for 60 min. The dishes were incubated overnight at 4˚C with diluted rabbit polyclonal antibody directed against mouse Ngfr (ab8875, 1:50; Abcam). On the following day, endogenous peroxidase was blocked with 3% H_2O_2 in methanol for 30 min. Biotinylated secondary antibodies were applied for 30 min at room temperature. Detection was carried out by using a Vectastain ABC Elite kit (Vector Laboratories) and the DAB system (Nichirei), as previously described.

Isolation of the basal cell from mouse primary cultured cells by magnetic cell sorting (MACS). MACS was carried out according to the manufacturer's protocol (Miltenyi Biotec GmbH, Germany). In brief, mouse primary cultured cells were tripsinized, centrifuged for 5 min at 1200 rpm, and then blocked with 0.5% BSA. The cells were incubated with monoclonal anti-mouse integrin b1 (CD29) antibody (diluted 1:50 in 0.5% BSA; BD Biosciences) for 30 min at 4˚C. After washing twice with 0.5% BSA, the cells were labeled with

anti-rat IgG antibody-microbeads (1:5; Miltenyi) for 15 min at 4˚C. Using the auto MACS system (Miltenyi), CD29-positive and -negative cells were recovered.

Laser-captured microdissection (LCM) and RNA preparation for RT-PCR. Mouse esophagus was embedded in TissueTek OCT medium (VWR Science) and snap-frozen in liquid nitrogen. The cryostat sections (8-μm) were laser-microdissected with a Pixcell II LCM system (Arcturus Engineering, Mountain View, CA).

Microarray analysis. Total RNA was isolated by suspending the cells in an Isogen lysis buffer (Nippon Gene, Toyama, Japan) followed by precipitation with isopropanol. The mRNA was amplified by an efficient method of high-fidelity mRNA amplification developed in our laboratory, called TALPAT (T7RNA polymerase promoter-attached, adaptor ligation-mediated, and PCR amplification followed by *in vitro* T7-transcription) (8). We used Mouse Expression Array 430A (Affymetrix, Santa Clara, CA) for analysis of mRNA expression levels corresponding to 22,690 transcripts. The procedures were conducted according to the supplier's protocols. Briefly, 10 μg of fragmented cRNA was hybridized to the microarrays in 200 μl of a hybridization cocktail at 45˚C for 16 h in a rotisserie oven set at 60 rpm. The arrays were then washed with a nonstringent wash buffer (6X SSPE) at 25˚C, followed by a stringent wash buffer [100 mM MES (pH 6.7), 0.1 M NaCl, and 0.01% Tween-20] at 50˚C, stained with streptavidin phycoerythrin (Invitrogen), washed again with 6X SSPE, stained with biotinylated anti-streptavidin IgG, followed by a second staining with streptavidin phycoerythrin and a third wash with 6X SSPE. The arrays were scanned using a GeneArray scanner (Affymetrix) at 3-μm resolution, and the expression value (average difference; AD) of each gene was calculated using GeneChip Analysis Suite version 4.0 software (Affymetrix). The mean of AD values in each experiment was 1000 to reliably compare variable multiple arrays. More than 2-fold overexpressed genes were selected by Microsoft Excel.

Reverse transcription-polymerase chain reaction (RT-PCR). Total RNA was isolated by suspending the cells in an Isogen lysis buffer (Nippon Gene) followed by precipitation with isopropanol. The mRNA was amplified by TALPAT. RT-PCR was carried out using primer sets designed for detecting the 3' side of cDNA of each gene. Primer sequences are shown in Table I. PCR was performed under conditions of 30-35 cycles of 3 steps of temperature, 95˚C for 1 min, 55˚C for 1 min, and 72˚C for 1 min, using the AccuPrime Taq DNA polymerase system (Invitrogen).

Results

The growth of the esophageal epithelium in mouse neonate. In humans (6,7), the lamina propria invaginates the epithelium, producing papillary structures. Hence, the basal layer is further divided into two types: one flat (the interpapillary basal layer, IBL) and one covering the papillae (the papillary basal layer, PBL) (Fig. 1). It has been reported that esophageal stem cells, displaying asymmetrical mitotic figures, may be localized to the IBL while transit amplifying cells may reside in the PBL (6,7). In contrast to humans, the mouse esophageal epithelium is progressively keratinized towards the luminal surface and consists of very thin layers of the epibasal cell. Furthermore, the mouse esophageal epithelium shows at most a quite short papillary structure. Therefore, the interpapillary basal cells, which contain the stem cells, may be present in relatively large numbers in the esophageal epithelium of mice as compared with humans. This characteristic may provide an advantage in the establishment of a primary culture system for studies on the cell differentiation processes from the stem cells to the terminally differentiated squamous cells.

While establishing a mouse esophageal epithelial cell culture system, we investigated the growth of the esophagus in the mouse neonates. To calculate the number of the basal cell, we stained Ngfr because the basal cell expressed Ngfr in adult mice as well as in adult humans (9) (Figs. 1 and 2A). Unexpectedly, in the mouse neonate, Ngfr was detected in the lamina propria (Fig. 2A, red arrows) but not in the basal cell (black arrows) 0 to 2 days after birth, although Ngfr then became detectable in the basal cells on days 3 to 9 after birth (Fig. 2A). We further investigated *Ngfr* mRNA expression in the basal cells of postnatal day 1 mice. In the esophagus, the basal cell is known to express integrins including Integrin-b1 (Itgb1), -a1 (Itga1), and -b4 (Itgb4) as well as Ngfr (10). Hence, we isolated the basal cells from mouse esophageal epithelium primary cultures by MACS with anti-Integrin-b1 (CD29) antibody. *Ngfr* mRNA was shown to be enriched together with mRNAs of the above Integrins by RT-PCR in a CD29-positive cell fraction (Fig. 2B). These results suggest that *Ngfr* mRNA is expressed in the basal cells on early postnatal days (0-2 days). Therefore, on such days, Ngfr protein may have been secreted by the basal cell, with the result that this protein was accumulated and detected in the lamina propria (Fig. 2A). This notion is supported by a previous report showing that the truncated and secreted form is produced from a post-translational modification of the intact, surface-bound form of the Ngfr protein (11).

Next, in three sections of the esophagus of the three young and adult 57BL/6J mice, we counted the number of basal cells as an indicator of esophageal epithelium growth. The number of basal cells was approximately 200 per horizontal section until 2 days after birth; 250 on postnatal day 3; 400 on day 9, and 600 in adult mice (Fig. 3A). Considering the circadian control of cell division, we investigated the expression of proliferating cell nuclear antigen (Pcna) in the esophagi of the neonates at the same time in the morning. As shown in Fig. 3B, a majority of Pcna-positive cells were basal cells. Consistent with the increase of the basal cells from postnatal day 3 (Fig. 3A), the rate of the Pcna-positive basal cells in postnatal day 3 mice significantly increased compared with that in the day 2 mice (Fig. 3B). These results suggest that the growth of the esophageal epithelium begins from postnatal day 3, and that the timing is consistent with that when Ngfr localizes to the basal cell membrane.

Increase of the basal cell number by Ngf treatment in in vitro mouse esophageal epithelium cultures. By the procedures described in the Materials and methods section, we first tried to culture mouse esophageal epithelium of the 57BL/6J mice on postnatal days 1 to 14 and at the adult stage (data not

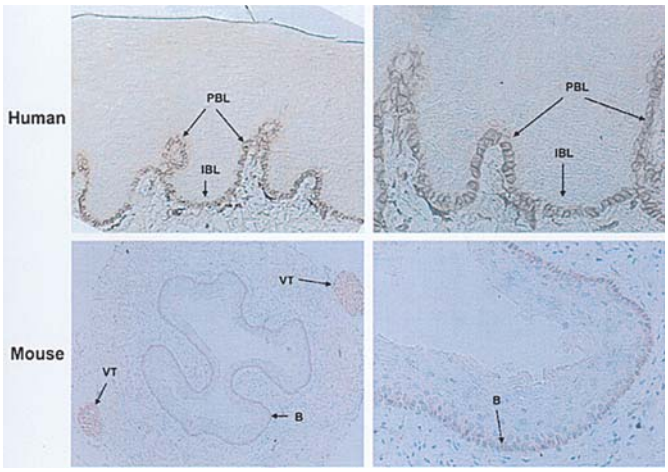

Figure 1. Expression of NGFR/Ngfr in the esophageal epithelium in adult humans and mice. Immunohistochemical analyses for NGFR/Ngfr shows that this receptor is localized in the basal cell membrane in adult humans (upper) and adult mice (lower). For tissues other than the epithelium, only the vagus nerve trunk expresses this receptor. BL, papillary basal cell; IBL, interpapillary basal cell; B, basal cell; VT, vagus nerve trunk. Left, magnification x100; right, magnification x200.

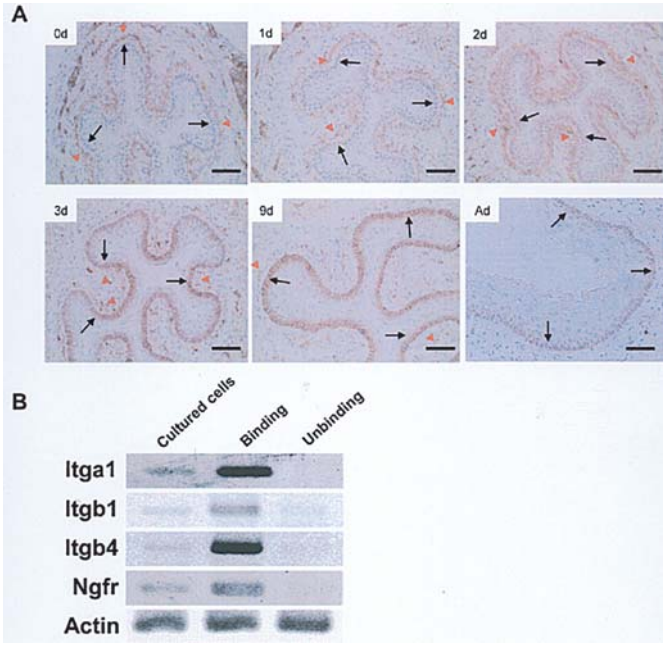

Figure 2. Expression of Ngfr protein and Ngfr mRNA in the basal cells in the neonatal mice. (A) Immunostaining of Ngfr in young mice (magnification x100). In mouse neonate, Ngfr was detected in the lamina propria (red arrows) but not in the basal cell (black arrows) 0 to 2 days after birth, while Ngfr was detected in the basal cell on days 3 to 9 after birth. 0d-9d, the postnatal 0-9 day mice; Ad, adult mice. Bar, 200 μm. (B) *Ngfr* mRNA expression in the basal cells of postnatal day 1 mice. In the esophagus, the basal cell is known to express Integrins including Integrin-b1 (Itgb1), -a1 (Itga1), and -b4 (Itgb4) as well as Ngfr. The basal cells from the esophageal epithelium primary cultures of postnatal day 1 mice are isolated by MACS with anti-Integrin b1 (CD29) antibody, and then RT-PCR is performed. *Ngfr* mRNA is enriched together with mRNAs of the above Integrins in a CD29-positive cell fraction. Binding, CD29-positive fraction; Unbinding, CD29-negative fraction.

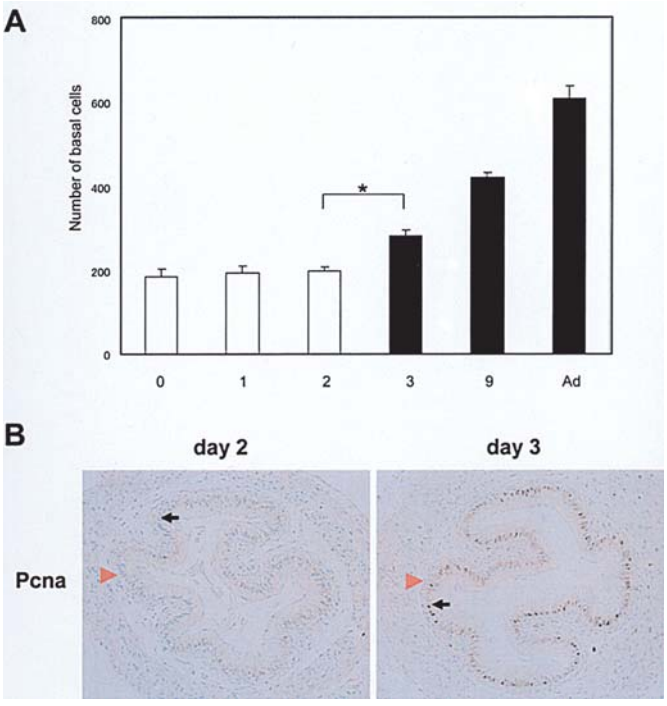

Figure 3. The growth of the esophageal epithelium in the mouse neonate. (A) The number of basal cells per horizontal section was counted for each postnatal day designated in abscissa. *Increase in the number of the basal cells on postnatal day 3 is statistically significant at $P<0.05$ as compared to that on postnatal day 2. (B) The rate of Pcna-positive basal and epibasal cells on postnatal day 2 mice significantly increased compared with that on day 3 mice (magnification x100). Black arrow, the basal cells; red arrow, the lamina propria.

shown). The cells were found to grow very well and form large colonies after 14 days in the culture of the esophageal epithelial cells isolated from the early postnatal days 1 to 7; however, in the culture derived from the postnatal day 8 to 14 epithelia, the cells decreased growth and formed small colonies. Furthermore, in the adult mice, the esophageal epithelial cells did not even form small colonies. Next, we characterized the primary cultures of the esophageal epithelium on early postnatal day 3 for 14 days (Fig. 4B). On day 1 after culture, a single cell was dominantly present (red arrowhead), and on days 2 to 4, the majority of colonies formed were small, composed of <10 cells that gave only a positive staining for a basal cell marker, cytokeratin 14 (Krt14) (7) (Fig. 4A and B). However, approximately half of the colonies became large, comprising 20-30 cells on days 5 to 6. The majority of the outer cells of the colonies gave a positive staining for Krt14, while that of the inner cells was positive for a differentiated cell marker, Krt10 (12,13) (Fig. 4A and B). Furthermore, on days 7 to 14, keratinized cells appeared in the inner layers of most of the colonies.

In this primary culture system of neonatal murine esophageal epithelial cells, the most important characteristics are that colonies containing Krt14-positive undifferentiated cells (basal cells) and Krt10-positive differentiated cells seem to be produced from a single basal cell, and that, until day 4 after culture, only the basal cell population increases in each colony. As described in the introduction, only the stem cells, which may be present in the basal cell layer, have the ability of self-renewal and asymmetric growth, while the progenitor cells (transit amplifying cells), which constitute most of the basal

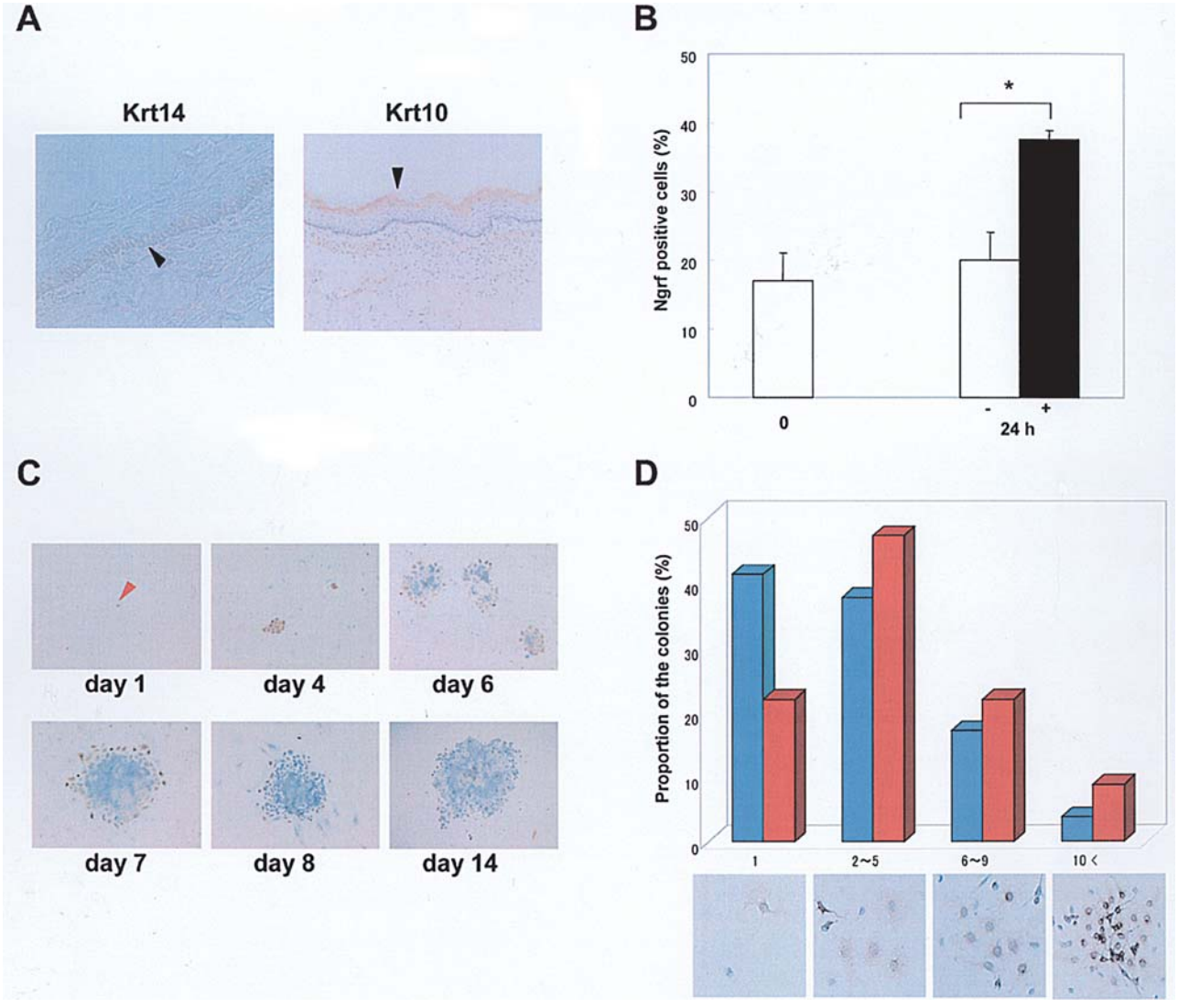

Figure 4. Characterization of the mouse primary esophageal epithelial cell culture. (A) Immunostaining of the differentiated and basal cell markers in the mouse esophageal epithelium (magnification x100). Cytokeratin 14 (Krt14) is stained in the basal cells, while Cytokeratin 10 (Krt10) is stained in the differentiated cells. (B) Immunostaining of Krt14 and Krt10 in the mouse primary esophageal epithelial cell culture (magnification x100). On day 1 after culture, most cells are present as a single isolated cell (red arrow). On early days (days 1-4), most cells in a small colony were positive for a basal cell marker, Krt14 (brown). On days 6 to 14, each colony became larger, and the majority of the 'outer' cells on the periphery of the colonies showed a positive staining for Krt14 (Brown), while the 'inner' cells in the central portion of the colonies showed a positive staining for a differentiated cell marker, Krt10 (Blue). Furthermore, keratinized cells appeared in the inner layers of most of the colonies. (C) The recombinant mouse Ngf was added to the primary cultures of the postnatal day 3 mice. *After 24 h, the number of Krt14-expressing cells in the Ngf-treated cultures significantly increased at $P<0.05$ compared with that in the untreated control. (D) The colonies enlarged after Ngf-treatment. Red, Ngf-treated; blue, untreated. Representative colonies (magnification x200) containing various numbers of Ngfr-positive cells are shown (lower): 1, one cell; 2-5, 2-5 cells; 6-9, 6-9 cells; >10, more than 10 cells, respectively.

cells, have no capacity for self-renewal. The characteristics of the primary cultures suggest that a symmetrical cell division, resulting in two daughters of the basal cells, preferentially occurred from day 1 to 4 after culture. From day 5 to 14, an asymmetrical cell division seems to occur preferentially, producing one basal and one differentiated cell, possibly through the epibasal daughter cell. Therefore, this esophageal epithelial cell culture system of the neonatal mice is useful for studies on the basal cell self-renewal and keratinocyte differentiation.

To examine the effect of Ngf in the basal cells, we added recombinant mouse Ngf to the primary cultures of the postnatal day 3 mice. After 24 h, the number of cells expressing Krt14 increased compared with that of the untreated control (Fig. 4C). Next, we stained another basal cell marker, Ngfr, and investigated the colony size. The colonies consisting of the Ngfr-positive cell were also observed to enlarge after Ngf-treatment for 24 h (Fig. 4D). These results suggest that Ngf may be required for basal cell growth and/or survival with the membrane localization of its receptor.

Expression change of other receptor genes in the basal cell during growth. To identify genes up-regulated in the basal cells after postnatal day 3, we performed microarray analysis of the primary cultured esophageal epithelial cells of postnatal day 4 and day 1 mice. Of 22,690 genes, 274 genes were identified as more than 2-fold up-regulated in the cultured cells of the postnatal day 4 mice (Table II). We found three genes, *roundabout homolog 1* (*Robo1*), *Egfr* and *Pdgfrb*, as the gene encoding growth factor receptor, which were highly

Table II. Gene candidates whose expression is up-regulated in the esophageal basal cells after postnatal day 3.

No.	Entrez gene ID	Gene symbol	Signal intensity day 1[a]	Signal intensity day 4[b]	Fold change day 4/day 1
1	12826	Col4a1	1[c]	2985	2984.6
2	22139	Ttr	1	2207	2207.2
3	20760	Sprr2f	1	2017	2016.8
4	66060	0610010O12Rik	1	1315	1315.2
5	19296	Pvt1	1	1296	1296.4
6	80837	Rhoj	1	1272	1271.7
7	20815	Srpk1	1	1257	1257.4
8	17075	Tacstd1	1	1228	1228.0
9	20305	Ccl6	1	1200	1199.5
10	66434	2010003O02Rik	1	1119	1118.6
11	22643	Zfp101	1	1083	1082.9
12	235674	MGC29978	1	1032	1031.5
13	12925	Crip1	1	1000	999.7
14	85031	Pla1a	1	990	989.9
15	225283	BC021395	1	981	981.4
16	18830	Pltp	1	954	953.8
17	83675	Bicc1	1	952	951.7
18	12642	Ch25h	1	939	938.5
19	66128	Mrps36	1	877	877.1
20	66601	2010002A20Rik	1	845	845.4
21	21804	Tgfb1i1	1	836	836.3
22	19335	Rab23	1	812	811.6
23	52123	Agpat5	1	805	805.1
24	14205	Figf	1	800	800.4
25	20842	Stag1	1	770	769.6
26	52535	D14Ertd209e	1	761	761.1
27	52357	D8Ertd594e	1	748	747.9
28	69875	Ndufa11	1	746	746.2
29	72415	Sgol1	1	744	744.0
30	21894	Tln1	1	733	732.7
31	16782	Lamc2	1	729	729.4
32	94227	Pi15	1	728	727.6
33	109225	Ms4a7	1	723	722.5
34	20758	Sprr2d	1	703	702.7
35	56043	Akr1e1	1	691	690.6
36	52443	Mrpl48	1	690	690.1
37	73826	Poldip3	1	690	689.6
38	15547	Htf9c	1	666	665.8
39	13436	Dnmt3b	1	655	654.7
40	21930	Tnfaip6	1	653	653.3
41	57814	Kcne4	1	653	652.5
42	227743	Mapkap1	1	639	638.8
43	74325	Cltb	1	638	637.7
44	11350	Abl1	1	637	636.8
45	12868	Cox8a	1	636	635.6
46	26949	Vat1	1	636	635.6
47	64929	Scel	1	616	616.4
48	228911	Sdccag33l	1	614	614.2
49	53421	Sec61a1	1	614	614.2
50	68936	1190017O12Rik	1	599	598.5
51	67198	2810022L02Rik	1	598	597.6
52	68494	1110011C06Rik	1	593	592.7
53	11857	Arhgdib	1	591	590.6
54	494448	Cbx6	1	574	574.0
55	14221	Fjx1	1	574	573.7
56	15374	Hn1	1	566	565.8
57	12870	Cp	1	564	563.5
58	12798	Cnn2	1	562	561.7
59	12550	Cdh1	1	554	553.9
60	54138	Sca10	1	552	551.5
61	11544	Adprh	1	548	547.5
62	17533	Mrc1	1	547	547.4
63	66448	Mrpl20	1	540	540.3
64	21346	Tagln2	1	540	539.8
65	74100	MGI:107562	1	537	536.9
66	67726	1810073G14Rik	1	532	531.5
67	26939	Polr3e	1	530	530.4
68	16956	Lpl	1	530	529.8
69	104806	Fancm	1	529	529.1
70	24030	Mrps12	1	529	529.1
71	102209	Snapc2	1	528	528.2
72	59042	Cope	1	525	524.9
73	16688	Krt2-6b	1	525	524.5
74	30794	Pdlim4	1	521	521.2
75	72388	Ripk4	1	511	510.9
76	68611	Mrpl28	1	509	508.5
77	217684	4933426M11Rik	1	506	505.5
78	105837	Mtbp	1	503	503.2
79	66208	Nenf	1	501	501.4
80	16687	Krt2-6a	164	4166	25.4
81	109620	Dsp	148	1953	13.2
82	217258	Abca8a	760	8330	11.0
83	11668	Aldh1a1	539	5578	10.3
84	17313	Mgp	3382	23271	6.9
85	66695	Aspn	505	3088	6.1
86	20210	Saa3	3060	17697	5.8
87	116903	Calcb	237	1365	5.8
88	22061	Trp63	117	635	5.4
89	68659	1110032E23Rik	640	3302	5.2
90	23794	Adamts5	604	3066	5.1
91	66607	Ms4a4d	1266	6393	5.1
92	26388	Ifi202b	510	2481	4.9
93	56429	Dpt	3685	17070	4.6
94	117167	Steap4	2496	11485	4.6
95	15483	Hsd11b1	914	4119	4.5
96	53603	Tslp	510	2219	4.4
97	13479	Dpep1	3131	13405	4.3
98	216616	Efemp1	167	690	4.1
99	71145	Scara5	406	1623	4.0
100	74175	2300002G24Rik	385	1506	3.9
101	103250	D130043N08Rik	652	2544	3.9
102	66693	4631408O11Rik	3760	14564	3.9
103	67513	2610002J02Rik	174	672	3.9
104	14012	Eva1	214	825	3.9
105	50764	Fbxo15	160	604	3.8
106	77125	9230117N10Rik	1406	5292	3.8
107	11475	Acta2	4731	17691	3.7
108	227753	Gsn	4076	14926	3.7
109	14219	Ctgf	8112	29621	3.7
110	67458	1200007D18Rik	1646	5996	3.6
111	57349	Cxcl7	487	1742	3.6

Table II. Continued.

Table II. Continued.

No.	Entrez gene ID	Gene symbol	Signal intensity day 1[a]	Signal intensity day 4[b]	Fold change day 4/day 1
112	20308	Ccl9	1067	3803	3.6
113	68713	Ifitm1	317	1127	3.6
114	20363	Sepp1	3182	11272	3.5
115	14066	F3	855	3002	3.5
116	21817	Tgm2	2773	9708	3.5
117	20198	S100a4	154	534	3.5
118	12814	Col11a1	306	1058	3.5
119	18542	Pcolce	922	3176	3.4
120	83691	Crispld1	499	1688	3.4
121	11657	Alb1	207	682	3.3
122	260409	Cdc42ep3	724	2367	3.3
123	22359	Vldlr	193	621	3.2
124	211623	Plac9	848	2702	3.2
125	11468	Actg2	174	552	3.2
126	26900	Ddx3y	434	1348	3.1
127	269831	Tspan12	353	1094	3.1
128	68195	Rnaset2	1541	4726	3.1
129	18596	Pdgfrb	692	2084	3.0
130	231507	Plac8	2334	6984	3.0
131	17190	Mbd1	318	949	3.0
132	16010	Igfbp4	837	2454	2.9
133	20750	Spp1	1646	4824	2.9
134	16525	Kcnk1	217	626	2.9
135	140742	Sesn1	876	2500	2.9
136	14062	F2r	2695	7679	2.8
137	193385	6330500D04Rik	548	1553	2.8
138	24010	Ik	3079	8670	2.8
139	18741	Pitx2	825	2303	2.8
140	16819	Lcn2	820	2287	2.8
141	20315	Cxcl12	2221	6181	2.8
142	101351	A130022J15Rik	341	947	2.8
143	11746	Anxa4	3609	9800	2.7
144	75746	Morc4	615	1647	2.7
145	226778	Mark1	280	749	2.7
146	231238	2310045A20Rik	376	1006	2.7
147	74055	Plce1	584	1561	2.7
148	67454	1200009F10Rik	947	2505	2.6
149	18805	Pld1	277	727	2.6
150	15228	Foxg1	4190	10956	2.6
151	23876	Fbln5	744	1943	2.6
152	70717	6330406I15Rik	1104	2806	2.5
153	67041	Oxct1	1054	2650	2.5
154	11522	Adh1	8275	20776	2.5
155	12834	Col6a2	5465	13680	2.5
156	110460	Acat2	3936	9827	2.5
157	64058	Perp	2013	4989	2.5
158	231207	Cpeb2	505	1241	2.5
159	11982	Atp10a	514	1262	2.5
160	192216	Tm4sf10	2236	5452	2.4
161	66214	1190002H23Rik	377	919	2.4
162	226251	Ablim1	370	900	2.4
163	12156	Bmp2	208	504	2.4
164	109552	Sri	218	527	2.4
165	58809	Rnase4	1802	4357	2.4
166	106264	0610012G03Rik	229	553	2.4
167	16885	Limk1	401	964	2.4

Table II. Continued.

No.	Entrez gene ID	Gene symbol	Signal intensity day 1[a]	Signal intensity day 4[b]	Fold change day 4/day 1
168	13506	Dsc2	1119	2683	2.4
169	65255	Asb4	236	564	2.4
170	19012	Ppap2a	1704	4057	2.4
171	66373	Lsm5	1856	4373	2.4
172	55990	Fmo2	445	1048	2.4
173	16952	Anxa1	12651	29731	2.4
174	12369	Casp7	320	749	2.3
175	19075	Prim1	2170	5051	2.3
176	381066	BC049807	924	2150	2.3
177	58801	Pmaip1	994	2292	2.3
178	14560	Gdf10	3563	8204	2.3
179	12974	Cs	226	519	2.3
180	67830	Rer1	255	584	2.3
181	21826	Thbs2	1822	4170	2.3
182	67951	Tubb6	447	1022	2.3
183	100198	H6pd	3383	7721	2.3
184	56744	Cxcl4	2967	6765	2.3
185	66508	2400001E08Rik	2399	5455	2.3
186	320712	D930038M13Rik	268	607	2.3
187	16987	Lss	321	726	2.3
188	17110	Lzp-s	1065	2395	2.2
189	13803	Enc1	1791	4000	2.2
190	14701	Gng12	2388	5331	2.2
191	14137	Fdft1	1385	3087	2.2
192	231532	Arhgap24	1411	3143	2.2
193	319953	Ttll1	272	605	2.2
194	21898	Tlr4	984	2185	2.2
195	19288	Ptx3	5650	12541	2.2
196	20411	Sorbs1	1556	3443	2.2
197	17181	Matn2	707	1558	2.2
198	210766	MGI:2389572	361	792	2.2
199	20393	Sgk	8914	19571	2.2
200	67267	2900010M23Rik	297	648	2.2
201	67097	Rps10	1219	2649	2.2
202	50770	Atp11a	1011	2193	2.2
203	13178	Dck	526	1137	2.2
204	13649	Egfr	665	1432	2.2
205	68198	Ndufb2	736	1583	2.2
206	14873	Gsto1	4587	9817	2.1
207	13429	Dnm1	534	1139	2.1
208	14866	Gstm5	379	806	2.1
209	76933	Ifi27	380	808	2.1
210	21810	Tgfbi	1563	3324	2.1
211	22183	U2af1-rs1	611	1293	2.1
212	71777	Ing3	349	738	2.1
213	110454	Ly6a	2931	6181	2.1
214	11796	Birc3	3755	7918	2.1
215	74617	Scpep1	4490	9460	2.1
216	70316	Ndufab1	2131	4488	2.1
217	380928	Lmo7	584	1229	2.1
218	17750	Mt2	11888	24924	2.1
219	192232	Hps4	271	568	2.1
220	50706	Postn	11165	23316	2.1
221	75751	Ipo4	428	890	2.1
222	50887	Nsbp1	1559	3243	2.1
223	16948	Lox	21373	44425	2.1

Table II. Continued.

No.	Entrez gene ID	Gene symbol	Signal intensity day 1[a]	Signal intensity day 4[b]	Fold change day 4/day 1
224	12393	Runx2	1313	2727	2.1
225	75619	2810421I24Rik	977	2025	2.1
226	14605	Tsc22d3	1272	2632	2.1
227	12494	Cd38	736	1522	2.1
228	214384	Myocd	387	801	2.1
229	70717	6330406I15Rik	429	886	2.1
230	14758	Gpm6b	5045	10427	2.1
231	494504	Apcdd1	360	744	2.1
232	13056	Cyb561	705	1456	2.1
233	67005	Polr3k	1715	3533	2.1
234	13602	Sparcl1	248	510	2.1
235	18032	Nfix	795	1632	2.1
236	53614	Reck	2918	5990	2.1
237	11745	Anxa3	7875	16160	2.1
238	101476	Plekha1	2092	4287	2.0
239	70536	Qpct	905	1852	2.0
240	66152	1110020P15Rik	252	515	2.0
241	192216	Tmem47	779	1587	2.0
242	12825	Col3a1	2757	5618	2.0
243	17448	Mdh2	1510	3076	2.0
244	17846	Commd1	703	1430	2.0
245	59005	1810017G16Rik	505	1027	2.0
246	11504	Adamts1	6682	13595	2.0
247	57342	Parva	406	825	2.0
248	11842	Arf3	1695	3427	2.0
249	12235	Bub1	940	1897	2.0
250	16007	Cyr61	601	1212	2.0
251	67217	2810055F11Rik	256	517	2.0
252	15122	Hba-a1	1256	2524	2.0
253	51869	Rif1	364	732	2.0
254	16009	Igfbp3	1964	3944	2.0
255	211739	BC027127	529	1060	2.0
256	22004	Tpm2	6920	13819	2.0
257	11489	Adam12	1700	3394	2.0
258	15959	Ifit3	1114	2219	2.0
259	353208	2810021G02Rik	784	1555	2.0
260	69706	Ppil5	655	1299	2.0
261	18783	Pla2g4a	4337	8596	2.0
262	12702	Socs3	998	1977	2.0
263	17748	Mt1	35272	69789	2.0
264	67204	Eif2s2	5698	11262	2.0
265	19366	Rad54l	254	502	2.0
266	21412	Tcf21	408	806	2.0
267	15958	Ifit2	1526	3011	2.0
268	56309	Mycbp	267	527	2.0
269	19242	Ptn	1268	2500	2.0
270	14190	Fgl2	444	874	2.0
271	19876	Robo1	798	1572	2.0
272	67732	4833421E05Rik	513	1010	2.0
273	11534	Adk	5483	10780	2.0
274	67054	Paics	4279	8394	2.0

[a]Day 1, the cultured cells in the postnatal day 1 mice; [b]day 4, those in the postnatal day 4 mice. [c]In the signal intensity of day 1, 1 means undetectable (absence).

expressed in the esophageal epithelial cell primary culture of the postnatal day 4 mice compared with that of the postnatal day 1 mice. Since the primary cultured cells were prepared on day 2 of the primary culture, they primarily consisted of the basal cells described above. Therefore, it was expected that these three receptor genes would be highly expressed in the basal cells of the postnatal day 4 mice compared with that of the postnatal day 1 mice. For confirmation, we prepared RNA samples from two specimens: one (B) contained the basal cells, and the other (D+E) contained both the epibasal cells and the differentiated squamous cells by LCM (Fig. 5A). We then performed RT-PCR after amplification of a small amount of RNA (10-20 ng) by TALPAT (8). The mRNA of a basal cell marker gene *Krt14* was detected preferentially in specimen B, demonstrating that the target cells were effectively enriched by LCM. Both *Pdgfrb* and *Egfr* were expressed highly in specimen B of the postnatal day 4 mice compared with that of the postnatal day 1 mice (Fig. 5B). Thus, over-expression of *Pdgfrb* and *Egfr* is associated with the timing of accelerated growth of the esophageal epithelium in young mice.

Discussion

We discovered a unique phenomenon that the growth of the esophageal epithelium shows a remarkable activation point around postnatal day 3 in mice. In mammals, the neonate ingests breast milk very soon after birth, and then is infected orally with microorganisms through both lactation and other maternal care. This delayed start system may provide time for acquiring immunoresponsibility against microorganisms. Expressional and functional analyses of Toll-like receptors in young mice will be an interesting project in the future. To date, it is not known why growth is delayed and whether the same phenomenon occurs in humans. However, our finding provides a new experimental model for studies on self-renewal of esophageal epithelial stem cells.

Esophageal squamous cell carcinoma has a poor prognosis because of frequent metastasis to the lymph nodes and lungs (14-16). There is no radical therapy for patients with metastases. Studies on the molecular mechanisms of self-renewal of adult stem cells is quite important for understanding cancer cell growth and/or cancer stem cell growth. In the self-renewal of hematopoietic stem cells, the signaling of Wnt (17-20), Notch (21-23), and HoxB4 (24,25) is reported to be involved. In the neural stem or precursor cells, Bmi1 has been reported to have a critical role (26). Only the hedgehog signaling pathway has been involved in the self-renewal of a variety of organs including the brain (27,28), lung (29), pancreas (30), bone (31), and skin (32). In the stomach, Shh and Dhh expression have been shown to be greatest at the pit-gland transition and restricted to the parietal cells (33,34), while Ihh was expressed in the pit cells (34). Although the hedgehog signaling pathway acts as a polarizing signal for bi-directional differentiation in the stomach (33,34), it remains unknown whether this pathway plays a role in maintaining stem or precursor cells, owing to the lack of an *in vitro* culture system for expansion of those cells. In the esophagus, hedgehog signal activation itself is unclear (35). Here we report that NGF signaling is a candidate for the self-renewal of the esophageal epithelial stem cell.

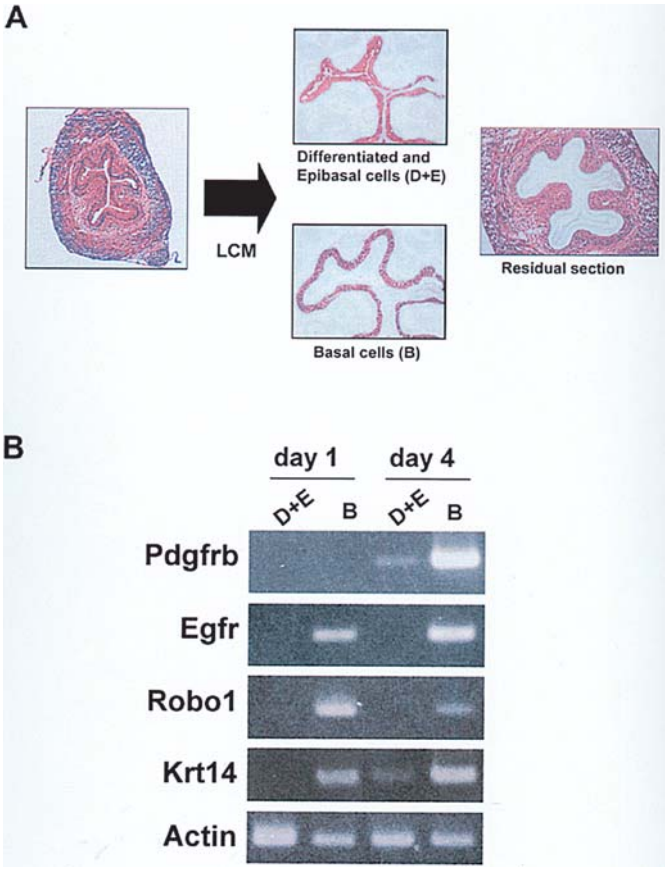

Figure 5. Expressional change of other receptor genes in the basal cell during growth. (A) Two different specimens, one (B) contained the basal cells, and the other (D+E) contained both the differentiated squamous cells and the epibasal cells, were prepared by laser-captured microdessection. (B) RT-PCR of *Robo1*, *Pdgfrb* and *Egfr* in the RNA samples from the two specimens. *Pdgfrb* and *Egfr* mRNAs were expressed at a higher level in the specimen B of postnatal day 4 mice than in that of the postnatal day 1 mice.

Consistent with the overexpression of *Egfr* and *Pdgfrb* in postnatal day 4 mice, Egf is known to be an essential growth factor for maintaining squamous cell cultures in the absence of serum, and Pdgf has also been reported to maintain the small side population, which is enriched for stem cells, in the C6 glioma cell line (2). These two growth factor receptor genes could be required for the basal cell self-renewal in the esophagus. Our extensive gene list and the present mouse primary culture system can contribute to studies on the self-renewal of the basal cells and keratinocyte differentiation in the esophagus.

Expression analysis of receptor genes in laser-captured cells revealed that *Robo1* and *Egfr* are expressed in the basal cells in the mouse neonates but not in those in adult mice (Fig. 5B). This suggests that the signal transduction through some receptors acts on the stem cells only in the growing stage. Therefore, *in situ* expression analysis by laser-captured basal cells is thought to be very important. Consistent with other reports (36-42), the TALPAT, which was used in RNA amplification of a very small amount of the laser-captured cells and the primary cultured cells (Fig. 5 and Table II), is thereby confirmed in its efficiency and high-fidelity. This method should be applied to the *in situ* expression analysis in the mouse neonates and adult mice in the future.

Acknowledgments

This work was supported in part by the program for promotion of Fundamental Studies in Health Sciences of the National Institute of Biomedical Innovation, in part by a Grant-in-Aid for the Third Comprehensive 10-Year Strategy for Cancer Control and for Cancer Research (16-15) from the Ministry of Health, Labour and Welfare of Japan, and in part by a research grant of the Princess Takamatsu Cancer Research Fund. H.D., N.I., and M.S. were awardees of research resident fellowships from the Foundation for Promotion of Cancer Research.

References

1. Al-Hajj M, Wicha MS, Benito-Hernandez A, Morrison SJ and Clarke MF: Prospective identification of tumorigenic breast cancer cell. Proc Natl Acad Sci USA 100: 3983-3988, 2003.
2. Kondo T, Setoguchi T and Taga T: Persistence of a small sub-population of cancer stem-like cells in the C6 glioma cell line. Proc Natl Acad Sci USA 101: 781-786, 2004.
3. Singh SK, Hawkins C, Clarke ID, Squire JA, Bayanl J, Hide T, Henkelman RM, Cusimano MD and Dirks PB: Identification of human brain tumour initiating cells. Nature 432: 396-401, 2004.
4. Huntly BJP and Gilliland DG: Leukaemia stem cell and the evolution of cancer-stem-cell research. Nat Rev Cancer 5: 311-321, 2005.
5. Kim CFB, Jackson EL, Woolfender AE, Lawrence S, Badar I, Vogel S, Crowley D, Bronson RT and Jacks T: Identification of bronchioalveolar stem cells in normal lung and lung cancer. Cell 121: 823-835, 2005.
6. Seery JP and Watt FM: Asymmetric stem-cell divisions define the architecture of human oesophageal epithelium. Curr Biol 10: 1447-1450, 2000.
7. Seery JP: Stem cell of the oesophageal epithelium. J Cell Science 115: 1783-1789, 2002.
8. Aoyagi K, Tatsuta T, Nishigaki M, Akimoto S, Tanabe C, Omoto Y, Hayashi S, Sakamoto H, Sakamoto M, Yoshida T, Terada M and Sasaki H: A faithful method for PCR-mediated global mRNA amplification and its integration into microarray analysis on laser-captured cells. Biochem Biophys Res Commun 300: 915-920, 2003.
9. Okumura T, Shimada Y, Imamura M and Yasumoto S: Neurotrophin receptor $p75^{NTR}$ characterizes human esophageal keratinocyte stem cell *in vitro*. Oncogene 22: 4017-4026, 2003.
10. Dobson H, Pignatelli M, Hopwood D and D'Arrigo C: Cell adhesion molecules in oesophageal epithelium. Gut 35: 1343-1347, 1994.
11. Barker PA, Miller FD, Large TH and Murphy RA: Generation of the truncated form of the nerve growth factor receptor by rat schwann cells. J Biol Chem 266: 19113-19119, 1991.
12. Squier CA and Kremer MJ: Biology of oral mucosa and esophagus. J Natl Cancer Inst Monogr 29: 7-15, 2001.
13. Banks-Schlegel S and Green H: Involucrin synthesis and tissue assembly by keratinocytes in natural and cultured human epithelia. J Cell Biol 90: 732-737, 1981.
14. Osugi H, Takemura M, Higashino M, Takada N, Lee S, Ueno M, Tanaka Y, Fukuhara K, Hashimoto Y, Fujiwara Y and Kinoshita H: Causes of death and pattern of recurrence after esophagectomy and extended lymphadenectomy for squamous cell carcinoma of the thoracic esophagus. Oncol Rep 10: 81-87, 2003.
15. Lee SJ, Lee KS, Yim YJ, Kim TS, Shim YM and Kim K: Recurrence of squamous cell carcinoma of the oesophagus after curative surgery: rates and patterns on imaging studies correlated with tumour location and pathological stage. Clinic Radiol 60: 547-554, 2005.
16. Motoyama S, Kitamura M, Saito R, Maruyama K, Okuyama M and Ogawa J: Outcome and treatment strategy for mid- and lower- thoracic esophageal cancer recurring locally in the lymph nodes of the neck. World J Surg 30: 191-198, 2006.
17. Reya T, Duncan AW, Ailles L, Domen J, Scherer DC, Willert K, Hintz L, Nusse R and Weissman IL: A role for Wnt signaling in self-renewal of haematopoietic stem cells. Nature 423: 409-414, 2003.

18. Muller-Tidow C, Steffen B, Cauvet T, Tickenbrock L, Ji P, Diederichs S, Sargin B, Kohler G, Stelljes M, Puccetti E, Ruthardt M, deVos S, Hiebert SW, Koeffler HP, Berdel WE and Serve H: Translocation products in acute myeloid leukemia activate the Wnt signaling pathway in hematopoietic cells. Mol Cell Biol 24: 2890-2904, 2004.
19. Zheng X, Beissert T, Kukoc-Zivojnov N, Puccetti E, Altshmied J, Strolz C, Boehrer S, Gul H, Schneider O, Ottmann OG, Hoelzer D, Henschler R and Ruthardt M: Gamma-catenin contributes to leukemogenesis induced by AML-associated translocation products by increasing the self-renewal of very primitive progenitor cells. Blood 103: 3535-3543, 2004.
20. Reya T and Clevers H: Wnt signaling in stem cells and cancer. Nature 434: 843-850, 2005.
21. Duncan AW, Rattis FM, DiMascio LN, Congdon KL, Pazianos G, Zhao C, Yoon K, Cook JM, Willert K, Gaiano N and Reya T: Integration of Notch and Wnt signaling in hematopoietic stem cell. Nat Immunol 6: 314-322, 2005.
22. Varnum-Finney B, Xu L, Brashem-Stein C, Nourigat C, Flowers D, Bakkour S, Pear WS and Bernstein ID: Pluripotent, cytokine-dependent, hematopoietic stem cells are immortalized by constitutive Notch1 signaling. Nat Med 6: 1278-1281, 2000.
23. Karanu FN, Murdoch B, Gallacher L, Wu DM, Koremoto M, Sakano S and Bhatia M: The notch ligand jagged-1 represents a novel growth factor of human hematopoietic stem cells. J Exp Med 192: 1365-1372, 2000.
24. Sauvageau G, Thorsteinsdottir U, Eaves CJ, Lawrence HJ, Largman C, Lansdorp PM and Humphries RK: Over expression of HOXB4 in hematopoietic cells causes the selective expansion of more primitive populations *in vitro* and *in vivo*. Genes Dev 9: 1753-1765, 1995.
25. Antonchuk J, Sauvageau G and Humphries RK: HOXB4-induced expansion of adult hematopoietic stem cells *ex vivo*. Cell 109: 39-45, 2002.
26. Valk-Lingbeek ME, Bruggeman SW and van Lohuizen M: Stem cells and cancer; the polycomb connection. Cell 118: 409-418, 2004.
27. Wechsler-Reya RJ and Scott MP: Control of neuronal precursor proliferation in the cerebellum by Sonic Hedgehog. Neuron 22: 103-114, 1999.
28. Palma V, Lim DA, Dahmane N, Sanchez P, Brionne TC, Herzberg CD, Gitton Y, Carleton A, Alvarez-Buylla A, Ruiz I and Altaba A: Sonic hedgehog controls stem cell behavior in the postnatal and adult brain. Development 132: 335-344, 2005.
29. Watkins DN, Berman DM, Burkholder SG, Wang B, Beachy PA and Baylin SB: Hedgehog signaling within airway epithelial progenitors and in small-cell lung cancer. Nature 422: 313-317, 2003.
30. Kawahira H, Scheel DW, Smith SB, German MS and Hebrok M: Hedgehog signaling regulates expansion of pancreatic epithelial cells. Dev Biol 280: 111-121, 2005.
31. Wdwards PC, Ruggiero S, Fantasia J, Burakoff R, Moorji SM, Paric E, Razzano P, Grande DA and Mason JM: Sonic hedgehog gene-enhanced tissue engineering for bone regeneration. Gene Ther 12: 75-86, 2005.
32. Adolphe C, Narang M, Ellis T, Wicking C, Kaur P and Wainwright B: An *in vivo* comparative study of sonic, desert and Indian hedgehog reveals that hedgehog pathway activity regulates epidermal stem cell homeostasis. Development 131: 5009-5019, 2004.
33. Van den Brink GR, Hardwick JC, Tytgat GN, Brink MA, Ten Kate FJ, Van Deventer SJ and Peppelenbosch MP: Sonic hedgehog regulates gastric gland morphogenesis in man and mouse. Gastroenterology 121: 317-328, 2001.
34. Fukaya M, Isohata N, Ohta H, Aoyagi K, Ochiya T, Saeki N, Yanagihara K, Nakanishi Y, Taniguchi H, Sakamoto H, Shimoda T, Nimura Y, Yoshida T and Sasaki H: Hedgehog signal activation in gastric pit cell and diffuse type gastric cancer. Gastroenterology 131: 14-29, 2006.
35. Lees C, Howie S, Sartor RB and Satsangi J: The hedgehog signaling pathway in the gastrointestinal tract: implications for development, homeostasis, and disease. Gastroenterology 129: 1696-1710, 2005.
36. Mori K, Aoyagi K, Ueda T, Danjoh I, Tsubosa Y, Yanagihara K, Matsuno Y, Sasako M, Sakamoto H, Mafune K, Kaminishi M, Yoshida T, Terada M and Sasaki H: Highly specific marker genes for detecting minimal gastric cancer cells in cytology negative peritoneal washings. Biochem Biophys Res Commun 313: 931-937, 2004.
37. Kobayashi K, Nishioka M, Kohno T, Nakamoto M, Maeshima A, Aoyagi K, Sasaki H, Takenoshita S, Sugimura H and Yokota J: Identification of genes whose expression is upregulated in lung adenocarcinoma cells in comparison with type II alveolar cells and bronchiolar epithelial cells *in vivo*. Oncogene 23: 3089-3096, 2004.
38. Nishigaki M, Aoyagi K, Donjoh I, Fukaya M, Yanagihara K, Sakamoto H, Yoshida T and Sasaki H: Discovery of aberrant expression of R-RAS by cancer-linked DNA hypomethylation in gastric cancer using microarrays. Cancer Res 65: 2115-2124, 2005.
39. Tatsuta T, Mukaisho K-I, Sugihara H, Miwa K, Tani T and Hattori T: Expression of Cdx2 in early GRCL of barrett's esophagus induced in rats by duodenal reflux. Dig Dis Sci 50: 425-431, 2005.
40. Yamada K, Kano J, Tsunoda H, Yoshikawa H, Okubo C, Ishiyama T and Noguchi M: Phenotypic characterization of endometrial stromal sarcoma of the uterus. Cancer Sci 97: 106-112, 2006.
41. Nakamura N, Kobayashi K, Nakamoto M, Kohno T, Sasaki H, Matsuno Y and Yokota J: Identification of tumor markers and differentiation markers for molecular diagnosis of lung adenocarcinoma. Oncogene (in press).
42. Nygaard V and Hovig E: Options available for profiling small samples: a review of sample amplification technology when combined with microarray profiling. Nucleic Acids Res 34: 996-1014, 2006.